



Published in final edited form as:

Pancreas. 2013 August ; 42(6): 937–943. doi:10.1097/MPA.0b013e318287ce21.

Repeatability of ⁶⁸Ga-DOTATOC PET Imaging in Neuroendocrine Tumors

Yusuf Menda, MD,

Department of Radiology, University of Iowa Carver College of Medicine, Iowa City, Iowa

Laura L. Boles Ponto, PhD,

Department of Radiology, University of Iowa Carver College of Medicine, Iowa City, Iowa

Michael K Schultz, PhD,

Department of Radiology, University of Iowa Carver College of Medicine, Iowa City, Iowa

Gideon K. D. Zamba, PhD,

Department of Biostatistics, University of Iowa College of Public Health, Iowa City, Iowa

G. Leonard Watkins, PhD,

Department of Radiology, University of Iowa Carver College of Medicine, Iowa City, Iowa

David L. Bushnell, MD,

Department of Radiology, University of Iowa Carver College of Medicine, Iowa City, Iowa

Mark T. Madsen, PhD,

Department of Radiology, University of Iowa Carver College of Medicine, Iowa City, Iowa

John J. Sunderland, PhD,

Department of Radiology, University of Iowa Carver College of Medicine, Iowa City, Iowa

Michael M. Graham, MD, PhD,

Department of Radiology, University of Iowa Carver College of Medicine, Iowa City, Iowa

Thomas M. O’Dorisio, MD, and

Department of Internal Medicine, University of Iowa Carver College of Medicine, Iowa City, Iowa

M. Sue O’Dorisio, MD

Department of Pediatrics, University of Iowa Carver College of Medicine, Iowa City, Iowa

Abstract

Objective—To evaluate the repeatability of ⁶⁸Ga-DOTA-D-Phe¹-Try³-Octreotide (⁶⁸Ga-DOTATOC) Positron Emission Tomography (PET) in neuroendocrine tumors.

Methods—Five patients with neuroendocrine tumors were imaged with ⁶⁸Ga-DOTATOC PET twice within 5 days. Maximum and average standardized uptake values (maxSUV and meanSUV) and kinetic parameters (K-Patlak and K-influx) of target lesions were measured. The repeatability of these measurements was investigated.

Results—47 target lesions were identified on whole body PET and 21 lesions on dynamic images. There was excellent repeatability with intraclass correlation coefficient of 0.99 for maxSUV, meanSUV and for K-Patlak and 0.85 for K-influx. The median absolute percent

Corresponding Author: Yusuf Menda, MD, Address: Department of Radiology, University of Iowa Hospitals and Clinics, 3858 JPP, 200 Hawkins Dr, Iowa City, IA, 52241, Phone: 319-356-3214, Fax: 319-356-2220, yusuf-menda@uiowa.edu.

Disclosures: The authors have no conflicts of interest or funding to disclose. This work was partly presented at the North American Neuroendocrine Tumor Society (NANETS) 2011 meeting in Minneapolis, Minnesota.

differences and the interquartile ranges (IQR) between two scans for maxSUV and meanSUV were 7.4% (IQR: 14.1%) and 9.3% (IQR: 10.6%), respectively. The median absolute percent differences for K-Patlak and K-influx were 12.5% (IQR: 12.6%) and 29.9% (IQR: 22.4%), respectively. The maxSUV of target lesions did not differ by more than 25% between two scans.

Conclusions— ^{68}Ga -DOTATOC PET imaging of neuroendocrine tumors is highly reproducible. A difference of more than 25% in maxSUV represents a change that is larger than the measurement error observed on repeated studies and should reflect a significant change in the biological character of the tumor.

Keywords

^{68}Ga -DOTATOC; PET; repeatability

Introduction

Indium-111 DTPA-D-Phe¹-octreotide (^{111}In -Octreotide; OctreoScan[®], Covidien) is the only FDA approved clinical imaging agent for somatostatin receptor scintigraphy of neuroendocrine tumors (NETs). It is particularly suited for well-differentiated NETs with high expression of sstr2 receptors. The sensitivity of ^{111}In -Octreotide is high (>75%) for carcinoid tumors and most pancreatic NETs(1); however it is diminished for tumors with lower expression of sstr2 receptors (such as insulinoma and medullary thyroid cancer) or small lesions with a low tumor-to-background ratio(2). Another potential disadvantage of ^{111}In -Octreotide is the relatively high radiation dose, which reaches an effective dose of 12 mSv (1.2 rem) for the recommended administered activity of 222MBq (6 mCi) in adults (2).

Positron emission tomography (PET) with fluorodeoxyglucose (FDG) has limited sensitivity in detection of well-differentiated neuroendocrine tumors(3). PET imaging with a new group of octreotide analogs labeled with Gallium-68 (^{68}Ga ; a generator product with a half-life of 68 minutes) and DOTA as chelator (^{68}Ga -DOTA-Octreotide analogs) have however shown highly promising results for detection of well differentiated neuroendocrine cancers. The most widely studied ^{68}Ga -DOTA-Octreotide analogs for PET imaging are ^{68}Ga -DOTA-D-Phe¹-Try³-Octreotide (^{68}Ga -DOTATOC), ^{68}Ga -DOTA-Tyr³-Thr⁸-octreotide (^{68}Ga -DOTA-TATE) and ^{68}Ga -DOTA-1-Nal³-octreotide (^{68}Ga DOTANOC). All of these radiopharmaceuticals target sstr2 in NETs with ^{68}Ga -DOTA-TATE demonstrating the highest affinity for sstr2 and ^{68}Ga -DOTANOC demonstrating the highest affinity for sstr3 and sstr5 receptors(4). Despite its lower affinity for sstr2, ^{68}Ga -DOTATOC PET has been shown to detect significantly more NET lesions compared to ^{68}Ga -DOTA-TATE(5). The potential advantages of ^{68}Ga -DOTA-Octreotide analogs over In-111 Octreotide include the higher resolution and accurate quantification of uptake achieved with PET compared to SPECT imaging and also the higher affinity of the ^{68}Ga -DOTA-Octreotide analogues for somatostatin receptor bearing tissues (6). Head-to-head comparisons of ^{68}Ga -DOTATOC and ^{111}In -Octreotide have demonstrated the higher sensitivity of ^{68}Ga -DOTATOC for the detection of neuroendocrine tumors (7–9). The radiation dosimetry of ^{68}Ga -DOTATOC is also favorable with an effective dose of 4.26 mSv (0.426 rem) for 185 MBq (5 mCi) of administered activity (10).

Although the utility of ^{68}Ga -DOTA-Octreotide analogs in detection of neuroendocrine tumors is now well recognized, their use in monitoring treatment response is less well established (11). To evaluate treatment response with ^{68}Ga -DOTA-Octreotide analogs, the repeatability of uptake measurements with these radiopharmaceuticals needs to be established. The objective of this study was to evaluate the repeatability of ^{68}Ga -DOTATOC

uptake in tumors as measured by standardized uptake value (SUV) and kinetic parameters in NET lesions as determined by imaging on two separate occasions.

Materials and Methods

Patient Characteristics

Five subjects with neuroendocrine tumors with widespread metastatic disease based on previous ^{111}In -Octreotide imaging and with plans for future peptide receptor radionuclide therapy (PRRT) were enrolled in this study. There were three males and two females with a mean age of 55 (range: 36–67). The primary tumors were midgut carcinoids in 3 patients, gastrinoma in one patient and carcinoid of unknown primary in one patient. The clinical and pathological features of each subject are summarized in Table 1. Each subject underwent two ^{68}Ga -DOTATOC PET scans within 5 days. All subjects were off long-acting release octreotide for 5 weeks prior to the scans and had no interval octreotide therapy between the two ^{68}Ga -DOTATOC PET scans. The study was approved by the University of Iowa Institutional Review Board (IRB) and Radioactive Drug Research Committee (RDRC) and each subject provided a signed informed consent.

^{68}Ga DOTATOC Synthesis

Synthesis of ^{68}Ga -DOTATOC was performed using an automated $^{68}\text{Ge}/^{68}\text{Ga}$ generator (IGG100, Eckert-Ziegler) coupled with a ModularLab PharmTracer fluid handling system (Eckert-Ziegler) adapted for methods similar to those described by Zhermosekov et al(12). A significant modification, which simplified the approach, involved the inclusion of the STRATA-XC cation exchange resin, which enabled the removal of a rinse step in the purification process. Further, adaptation of the method for the automated system enables daily production in a virtually hands free environment, which minimizes personnel dose to operators during the production process. Details of the methodology and automation are presented elsewhere (13,14). Briefly, ^{68}Ga was eluted with 6 mL 0.1 M hydrochloric acid (HCl) to an in-line cation exchange resin (STRATA-XC, Phenomenex), which retains ^{68}Ga . Purified ^{68}Ga is then eluted with 98% acetone/0.02 M HCl to a glass reaction vessel containing 21 nmoles (30 μg) DOTATOC (in 2 mL sodium acetate buffer, pH 4). Radiolabeling is carried out at 95 °C for 6 min. Acetone is removed by vent to waste during the radiolabeling step. Following radiolabeling, ^{68}Ga -DOTATOC is transferred to an in-line disposable C-18 cartridge (Strata-X, Phenomenex). Free ^{68}Ga is removed by saline rinse and pure ^{68}Ga -DOTATOC is eluted in 2 mL 1:1 95% ethanol:water to the product vial *via* a 0.22 μm sterilizing filter and diluted to approximately 7 mL with isotonic saline for injection. QC parameters were measured by standard techniques.

The decay-corrected radiochemical yield was 50–60%. Conservative estimates of specific activity and the amount of peptide injected per patient dose assume quantitative transfers of DOTATOC peptide. The estimated specific activity at end of synthesis, assuming quantitative transfer of DOTATOC was 26 ± 1 MBq/nmol and the radiochemical purity was $98 \pm 1\%$. Other quality control parameters (pH; filter integrity, acetone, ethanol, and endotoxins) were well within specifications. Specific activity at the time of injection was 17 ± 1 MBq/nmol and the amount of peptide per injected dose was estimated to be 16 ± 1 μg of DOTATOC.

^{68}Ga -DOTATOC PET-CT Imaging

Following the IV administration of 185 MBq (5mCi) of ^{68}Ga -DOTATOC, dynamic images of the chest or abdomen (i.e. centered over the target lesion) were obtained for 60 minutes (36 frames at 12 x 10sec/frame, 6 x 30sec/frame, 5 x 60 sec/frame, 5 x 2min/frame and 8 x 5 min/frame) on an ECAT EXACT HR+ PET scanner (Siemens Medical Solutions USA, Inc.)

operated in the 3-dimensional mode. A pre-injection transmission scan with a ^{68}Ge pin source was obtained for attenuation correction of dynamic images. Concurrent with dynamic imaging, venous blood samples were obtained at approximately 2, 4, 6, 10, 20 and 40 min after the injection of ^{68}Ga -DOTATOC. After the dynamic imaging was completed, the patient was transferred to a Siemens Biograph Duo PET-CT scanner (Siemens Medical Solutions USA, Inc.). A low-dose noncontrast whole body CT scan was acquired for attenuation correction and a PET scan was acquired from the base of the skull to the proximal thighs (7–8 bed positions). Dynamic PET and whole body PET-CT images were iteratively reconstructed; 2 iterations and 8 subsets with an 8-mm gaussian postprocessing filter for dynamic images and 4 iterations and 16 subsets with a 5-mm gaussian postprocessing filter for whole body PET-CT images.

Image Analysis

Dynamic PET Imaging Data—Time-activity curves (TACs) were determined for volumes-of-interest (VOIs) for lesions identified on the dynamic frames on the first and second PET scan. VOIs were generated based on 50% thresholding of the voxel with the highest activity. Arterial plasma input functions were generated from VOIs over major vessels (e.g., aorta) corrected for the whole blood/plasma ratio determined from analysis of venous blood samples. Pharmacokinetic parameters based on non-compartmental (i.e., K-Patlak derived from Patlak graphical analysis) and compartmental modeling (i.e., K-influx derived from a two-tissue compartment model) were calculated for each target volume of interest (VOI). VOI and pharmacokinetic analyses were performed using the PVIEW and PKIN tools of the PMOD Biomedical Image Quantification software package (version 3.3, PMOD Technologies LTD, Zurich, Switzerland).

Whole Body PET-CT Data—For each subject, up to a total of 10 target lesions and a maximum of 5 lesions per organ were identified that included all involved organs. If more than five lesions were present in one organ (such as liver, lymph nodes or bone), the lesions with the highest uptake of ^{68}Ga DOTATOC were selected for analysis. Maximum pixel standardized uptake values (maxSUV) and the average SUV based on volumes of interest (VOIs) created as described above (meanSUV) were calculated for all target lesions on scan 1 and scan 2.

Statistical Analysis

The repeatability of the measurements was investigated using *Bland-Altman plots* as a graphical assessment tool and the *intraclass correlation coefficient (ICC)* as a statistical quantifier. The ICC quantifies the correlation between two replicates from the same subject, and is a consistent measure of reproducibility confined between 0 and 1. Higher values of ICC correspond to smaller within subject measurement variability; meaning that measurements are less variable from one replicate to the next. $\text{ICC} < 0.4$ indicates a poor reproducibility, $0.4 < \text{ICC} < 0.75$ indicates fair to good reproducibility and $\text{ICC} > 0.75$ indicates excellent reproducibility. Statistical analyses were performed using MedCalc software (version 12.2.1.0; MedCalc Software, Mariakerke, Belgium).

The difference between the two scans for SUV and kinetic parameters were calculated by *percent difference and absolute percent difference* using the following equations:

$$\text{Percent Difference} = 100 \times \frac{\text{Scan 1} - \text{Scan 2}}{\text{AVG}(\text{Scan 1}, \text{Scan 2})}$$

$$\text{Absolute Percent Difference} = 100 \times \text{ABS} \left(\frac{\text{Scan 1} - \text{Scan 2}}{\text{AVG}(\text{Scan 1}, \text{Scan 2})} \right)$$

Results

The interval between two PET scans was 1–5 days (mean \pm SD: 2.2 ± 1.6 days). The first whole body PET-CT scans were obtained 69–85 min after injection of the radiopharmaceutical. Because an attempt was made to match the uptake time prior to whole body imaging between the scans, the uptake period for the second PET-CT scan did not differ by more than 3 minutes from that of the first scan for each subject. Forty-seven target lesions were identified on whole body scans; a representative subject with numerous lesions is shown in Figure 1. The target lesions included 13 liver lesions, 19 lesions in lymph node basins, 9 bone lesions, 2 lung lesions and 1 lesion each in the pancreas, ileum, peritoneum and heart. Dynamic imaging was not usable for quantitation in one subject due to significant motion; in the remaining 4 subjects 21 lesions were identified on both dynamic images, including 9 nodal lesions, 11 liver lesions and 1 lesion in the pancreas.

There was an excellent repeatability between the two scans for both standardized uptake values and kinetic parameters (Figure 2). The intraclass correlation coefficient (ICC) was 0.99 for maxSUV and meanSUV, 0.99 for K-patlak and 0.85 for K-influx. The average percent differences for SUV and kinetic parameters are presented in Table 2. There was a positive correlation between SUV (mean and max) and the absolute difference of SUV between two scans; however the absolute percentage difference showed no correlation with the magnitude of the SUV (Figure 3).

The absolute percent differences for the mean SUV, K-Patlak and K-influx did not follow a normal distribution based on D'Agostino-Pearson test ($p=0.0001$), whereas a borderline Gaussian distribution was noted for SUVmax ($p=0.07$). Therefore the medians of absolute percent differences were also calculated along with the interquartile range (IQR). The median absolute percent differences between two scans in max SUV-WB and mean SUV-WB were 7.4% (IQR: 14.1%) and 9.3% respectively (IQR: 10.6%). For the kinetic parameters, the median absolute percent differences for K-Patlak and K-influx were 12.5% (IQR: 12.6%) and 29.9% (IQR: 22.4%), respectively. Excluding one outlier (identified with Tukey outlier test), the maxSUV in any target lesion did not differ by more than 25% between two scans (Figure 4A). The variability was significantly higher with K-influx (Figure 4B).

Discussion

^{68}Ga labeled somatostatin analogs are currently only available as investigational radiopharmaceuticals in the United States. They are, however, used as a clinical imaging tool in Europe to stage and re-stage neuroendocrine tumors as well as to provide quantitative measurement of somatostatin receptor expression, a prognostic indicator of potential tumor response to octreotide therapy or peptide receptor radionuclide therapy (PRRT)(11). Our investigation demonstrates the excellent repeatability of quantitative uptake measurements with ^{68}Ga -DOTATOC in neuroendocrine tumors. Furthermore our results suggest that a change of more than 25% in tumor maximum SUV between two scans is greater than the measurement error of uptake and should therefore reflect a change in the biological character of the tumor.

Standardized uptake value (SUV) provides a snapshot of uptake at a predetermined time point. The uptake of ^{68}Ga -DOTATOC is however a dynamic process that depends on plasma clearance and initial receptor binding and internalization of the receptor-ligand complex, and displacement from the receptor and externalization, which can be described through pharmacokinetic analysis using a two-tissue compartment model(15). In our study, the pharmacokinetic parameters, K-influx, based on a two-compartment model, and the K-

Patlak, based on the non-compartmental graphical approach, exhibited higher average absolute percent differences and, in the case of K-influx, lower ICC, than the SUV-based metrics with ^{68}Ga DOTATOC. Pharmacokinetic analyses require an arterial plasma input function and tumor time-activity-curves (TACs) for the calculation of the parameter values. Noise in either the tumor TAC or the image-derived arterial input function (due to subject motion or poor count statistics) or model misspecification can adversely effect the parameter estimates. Parameters derived from non-compartmental fits (i.e., K-Patlak) are generally more robust than those derived from compartmental fits (i.e., K-influx) as was evidenced by the results in the present study.

Although PET imaging with ^{68}Ga labeled somatostatin analogs is used as a clinical tool for staging of neuroendocrine tumors, the data on its utility in monitoring treatment response are more limited and controversial. Gabriel et al. found no advantage of using ^{68}Ga -DOTATOC over conventional imaging with CT or MRI in the evaluation of treatment response after completion of all cycles of peptide receptor radionuclide therapy(16). In their study of 45 patients with available SUV information in the index lesion, 19 patients showed more than a 20% drop in SUVmax, however only 8 of these patients were in remission. On the other hand, 8 of 10 patients with greater than a 20% increase in SUV had stable or improving disease. It should be noted, however, that many patients in this study developed new sites of metastases during follow-up, qualifying them for progressive disease regardless of the change in uptake in the index lesion. In a subsequent study by Haug et al., the change in uptake of ^{68}Ga -DOTA-TATE in target lesions correlated with time to progression and improvement in clinical symptoms after PRRT, with the SUV ratio of tumor-to-spleen performing better than SUVmax, although splenic uptake may also be altered after PRRT(17). In these studies, the reponse evaluation was performed either after completion of all therapy cycles or 3 months after the first cycle. However, there may be significant changes already occurring in the tumor early after the first cycle of PRRT, which may help in the early prediction of therapy response. Comparison of the uptake of radiolabeled somatostatin analogues in the tumor may be potentially even more valuable early after the initial treatment cycle as morphological methods would not reflect the response or could even be potentially misleading due to radiation induced tumor swelling.

The repeatability of uptake of PET radiopharmaceuticals is an area of significant focus because of the increasing use of PET imaging in monitoring response to cancer therapy. The repeatability of Fluorodeoxyglucose (FDG) uptake in tumors was investigated in a recent metaanalysis by de Langen et al (18). This metaanalysis examined six previously published studies (19–23), which included five patient cohorts with a combined 234 tumors. A change of more than 20% and 1.2 units in meanSUV and a difference of more than 30% and 2 units in maxSUV were found to represent a true change rather than measurement error in the SUV in this analysis. The percent differences in our study for ^{68}Ga -DOTATOC are similar to those reported for FDG, however, the absolute differences are significantly higher with ^{68}Ga -DOTATOC(Figure 3 Bland-Altman curves) due to the extremely large range of SUVs observed with ^{68}Ga -DOTATOC. In our study, 3 lesions had maxSUV greater than 90 (up to 249) and an additional 5 lesions had maxSUV greater than 30, values which would be exceedingly rare with FDG. Therefore a percentage change in uptake should be a more reliable tool compared to the absolute difference to evaluate the change in ^{68}Ga -DOTATOC uptake.

The variability of tumor uptake of ^{68}Ga -DOTATOC may be the result of a number of factors that influence directly the uptake of the radiopharmaceutical or the measurement of the uptake. The specific activity of ^{68}Ga -DOTATOC, i.e. the ratio of the concentration of the radioactivity to the concentration of the unlabeled ligand (unlabeled octreotide) of the radiopeptide, may have a significant effect on the binding of the radioligand. The tumor

uptake of ^{68}Ga -DOTATOC initially increases with a larger amount of the unlabeled peptide due to receptor clustering induced by the ligand, however, with the administration of a higher mass of the unlabeled peptide, the uptake decreases because of saturation of the somatostatin receptors(24). The dose-dependent effect of cold octreotide on tumor uptake of ^{68}Ga -DOTATOC was demonstrated by Veliky et al, who reported enhanced tumor uptake of ^{68}Ga -DOTATOC after IV administration of 50 μg of unlabeled octreotide, but a decrease in ^{68}Ga -DOTATOC uptake with higher doses of octreotide administration (25). Although the specific activity of the administered dose of ^{68}Ga DOTATOC can be controlled, the specific activity of ^{68}Ga DOTATOC may be significantly reduced *in vivo* in patients, who receive therapeutic doses of unlabeled octreotide. Although all of our subjects treated with long-acting release octreotide were imaged 5 weeks after the last treatment dose, there may still be a slight difference in the blood octreotide levels between the two scans. In view of these observations, octreotide therapy should be either discontinued prior to ^{68}Ga -DOTATOC PET scans if performed for treatment monitoring purposes, or alternatively, both baseline and follow-up scans should be performed under the same dose of octreotide therapy. The higher plasma availability of ^{68}Ga -DOTATOC, as would be seen in patients with slower renal clearance, may also increase the tumor SUV. This may be an important factor to consider in response assessment after peptide receptor radionuclide therapy (PRRNT), a treatment that may cause a significant decline in renal function.

The variation of tumor uptake measurements observed in this study may also be due to subtle differences in the size and position of the volumes of interest (VOIs) with respect to the tumor tissue. With respect to VOI definition, each scan was treated as a unique entity, therefore, the 50% of maximum pixel value (within the area) was applied for each lesion in each scan. Small changes in the maximum pixel value, due to the uptake of tracer but also from technical issues such as tumor motion secondary to breathing artifacts or change in bowel position, will translate directly into variability in the maxSUV, but also, potentially, in the definition of the VOI and therefore, dually affect the meanSUV. Still both maxSUV and mean SUV showed excellent repeatability between two scans with interclass correlation coefficient of 0.99. Finally, the tumor uptake and its repeatability may vary depending on the uptake period. In our study, the tumor uptake of ^{68}Ga -DOTATOC continued to increase throughout the dynamic acquisition period of 60 minutes. Therefore, for comparison purposes using SUV with ^{68}Ga -DOTATOC, the uptake period should be as similar as possible between the baseline and follow-up scans, particularly if imaging is to be started at 60 min or earlier after the injection of the radiopharmaceutical. In longitudinal studies, SUVs should ideally be obtained after the tumor uptake reaches a plateau, which based on our observations would require an uptake period longer than 60 minutes for ^{68}Ga -DOTATOC.

Conclusions

^{68}Ga -DOTATOC PET imaging of neuroendocrine tumors is highly reproducible. These preliminary findings suggest that a difference of more than 25% in tumor maximum SUV between two scans represents a change that is larger than the measurement error observed on repeated studies and should reflect a significant change in the biological character of the tumor.

Acknowledgments

The authors wish to acknowledge the generous contributions from the Gregg and Ondene Mamikunnian Family and the Ride-for-the-Kids Foundation in obtaining the modular lab for the synthesis of ^{68}Ga -DOTATOC and the Carcinoid Cancer Awareness Network (CCAN) for their support with travel expenses of our patients.

References

1. Kwekkeboom DJ, Krenning EP, Scheidhauer K, et al. ENETS Consensus Guidelines for the Standards of Care in Neuroendocrine Tumors: somatostatin receptor imaging with (111)In-pentetretotide. *Neuroendocrinology*. 2009; 90:184–9. [PubMed: 19713709]
2. Balon HR, Brown TL, Goldsmith SJ, et al. The SNM Practice Guideline for Somatostatin Receptor Scintigraphy 2. 0. *J Nucl Med Technol*. 2011; 39:317–24. [PubMed: 22068564]
3. Kayani I, Bomanji JB, Groves A, et al. Functional imaging of neuroendocrine tumors with combined PET/CT using 68Ga-DOTATATE (DOTA-DPhe1, Tyr3-octreotate) and 18F-FDG. *Cancer*. 2008; 112:2447–55. [PubMed: 18383518]
4. Antunes P, Ginj M, Zhang H, et al. Are radiogallium-labelled DOTA-conjugated somatostatin analogues superior to those labelled with other radiometals? *Eur J Nucl Med Mol Imaging*. 2007; 34:982–93. [PubMed: 17225119]
5. Poeppel TD, Binse I, Petersenn S, et al. 68Ga-DOTATOC versus 68Ga-DOTATATE PET/CT in functional imaging of neuroendocrine tumors. *Journal of nuclear medicine: official publication, Society of Nuclear Medicine*. 2011; 52:1864–70.
6. Reubi JC, Schar JC, Waser B, et al. Affinity profiles for human somatostatin receptor subtypes SST1-SST5 of somatostatin radiotracers selected for scintigraphic and radiotherapeutic use. *Eur J Nucl Med*. 2000; 27:273–82. [PubMed: 10774879]
7. Buchmann I, Henze M, Engelbrecht S, et al. Comparison of 68Ga-DOTATOC PET and 111In-DTPAOC (Octreoscan) SPECT in patients with neuroendocrine tumours. *Eur J Nucl Med Mol Imaging*. 2007; 34:1617–26. [PubMed: 17520251]
8. Gabriel M, Decristoforo C, Kendler D, et al. 68Ga-DOTA-Tyr3-octreotide PET in neuroendocrine tumors: comparison with somatostatin receptor scintigraphy and CT. *J Nucl Med*. 2007; 48:508–18. [PubMed: 17401086]
9. Kowalski J, Henze M, Schuhmacher J, et al. Evaluation of positron emission tomography imaging using [68Ga]-DOTA-D Phe(1)-Tyr(3)-Octreotide in comparison to [111In]-DTPAOC SPECT. First results in patients with neuroendocrine tumors. *Mol Imaging Biol*. 2003; 5:42–8. [PubMed: 14499161]
10. Hartmann H, Zophel K, Freudenberg R, et al. Radiation exposure of patients during 68Ga-DOTATOC PET/CT examinations. *Nuklearmedizin*. 2009; 48:201–7. [PubMed: 19639164]
11. Virgolini I, Ambrosini V, Bomanji JB, et al. Procedure guidelines for PET/CT tumour imaging with 68Ga-DOTA-conjugated peptides: 68Ga-DOTA-TOC, 68Ga-DOTA-NOC, 68Ga-DOTA-TATE. *European journal of nuclear medicine and molecular imaging*. 2010; 37:2004–10. [PubMed: 20596866]
12. Zhernosekov KP, Filosofov DV, Baum RP, et al. Processing of generator-produced 68Ga for medical application. *J Nucl Med*. 2007; 48:1741–8. [PubMed: 17873136]
13. Mueller D, Klette I, Baum RP, et al. Simplified NaCl Based (68)Ga Concentration and Labeling Procedure for Rapid Synthesis of (68)Ga Radiopharmaceuticals in High Radiochemical Purity. *Bioconjug Chem*. 2012
14. Schultz MKMD, Baum RP, et al. Automated methods for routine production of gallium-68 labeled peptides. *Appl Rad Isot*. in press.
15. Koukouraki S, Strauss LG, Georgoulas V, et al. Evaluation of the pharmacokinetics of 68Ga-DOTATOC in patients with metastatic neuroendocrine tumours scheduled for 90Y-DOTATOC therapy. *Eur J Nucl Med Mol Imaging*. 2006; 33:460–6. [PubMed: 16437218]
16. Gabriel M, Oberauer A, Dobrozemsky G, et al. 68Ga-DOTA-Tyr3-octreotide PET for assessing response to somatostatin-receptor-mediated radionuclide therapy. *J Nucl Med*. 2009; 50:1427–34. [PubMed: 19690033]
17. Haug AR, Auernhammer CJ, Wangler B, et al. 68Ga-DOTATATE PET/CT for the early prediction of response to somatostatin receptor-mediated radionuclide therapy in patients with well-differentiated neuroendocrine tumors. *Journal of nuclear medicine: official publication, Society of Nuclear Medicine*. 2010; 51:1349–56.

18. de Langen AJ, Vincent A, Velasquez LM, et al. Repeatability of 18F-FDG Uptake Measurements in Tumors: A Metaanalysis. *Journal of nuclear medicine: official publication, Society of Nuclear Medicine*. 2012; 53:701–8.
19. Weber WA, Ziegler SI, Thodtmann R, et al. Reproducibility of metabolic measurements in malignant tumors using FDG PET. *Journal of nuclear medicine: official publication, Society of Nuclear Medicine*. 1999; 40:1771–7.
20. Velasquez LM, Boellaard R, Kollia G, et al. Repeatability of 18F-FDG PET in a multicenter phase I study of patients with advanced gastrointestinal malignancies. *Journal of nuclear medicine: official publication, Society of Nuclear Medicine*. 2009; 50:1646–54.
21. Nahmias C, Wahl LM. Reproducibility of standardized uptake value measurements determined by 18F-FDG PET in malignant tumors. *Journal of nuclear medicine: official publication, Society of Nuclear Medicine*. 2008; 49:1804–8.
22. Minn H, Zasadny KR, Quint LE, et al. Lung cancer: reproducibility of quantitative measurements for evaluating 2-[F-18]-fluoro-2-deoxy-D-glucose uptake at PET. *Radiology*. 1995; 196:167–73. [PubMed: 7784562]
23. Hoekstra CJ, Hoekstra OS, Stroobants SG, et al. Methods to monitor response to chemotherapy in non-small cell lung cancer with 18F-FDG PET. *Journal of nuclear medicine: official publication, Society of Nuclear Medicine*. 2002; 43:1304–9.
24. Breeman WA, de Blois E, Sze Chan H, et al. (68)Ga-labeled DOTA-peptides and (68)Ga-labeled radiopharmaceuticals for positron emission tomography: current status of research, clinical applications, and future perspectives. *Seminars in nuclear medicine*. 2011; 41:314–21. [PubMed: 21624565]
25. Velikyan I, Sundin A, Eriksson B, et al. In vivo binding of [68Ga]-DOTATOC to somatostatin receptors in neuroendocrine tumours--impact of peptide mass. *Nucl Med Biol*. 2010; 37:265–75. [PubMed: 20346866]

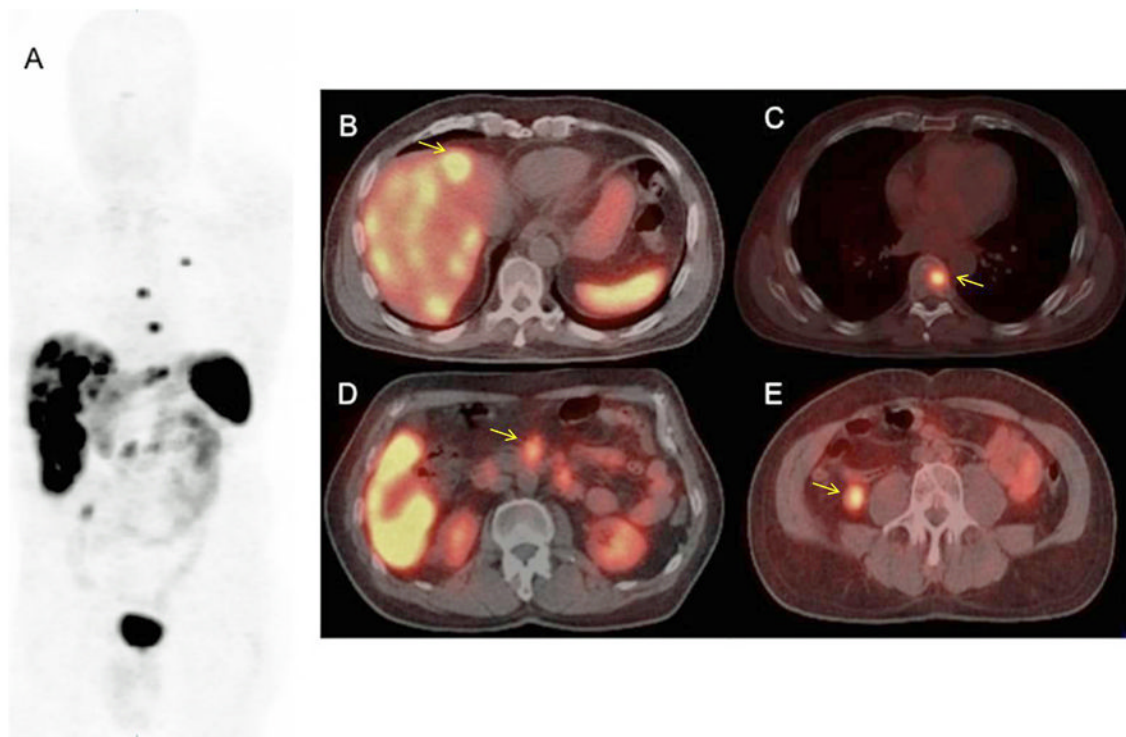


Figure 1. (A–E): ^{68}Ga -DOTATOC whole body PET (maximum intensity projection; Figure 1A) and select PET-CT images (Figure 1B–E) of a subject with widespread metastatic neuroendocrine tumor. Note the multiple liver lesions (Figure 1B; arrow), thoracic spine lesion (Figure 1C; arrow), paraaortic nodal lesions (Figure 1D; arrow) and an ileal small bowel lesion in the right lower quadrant (Figure 1E; arrow). The ileal primary lesion, which was subsequently confirmed surgically, was not detected prospectively on the ^{111}In -Octreotide scan obtained prior to ^{68}Ga -DOTATOC study.

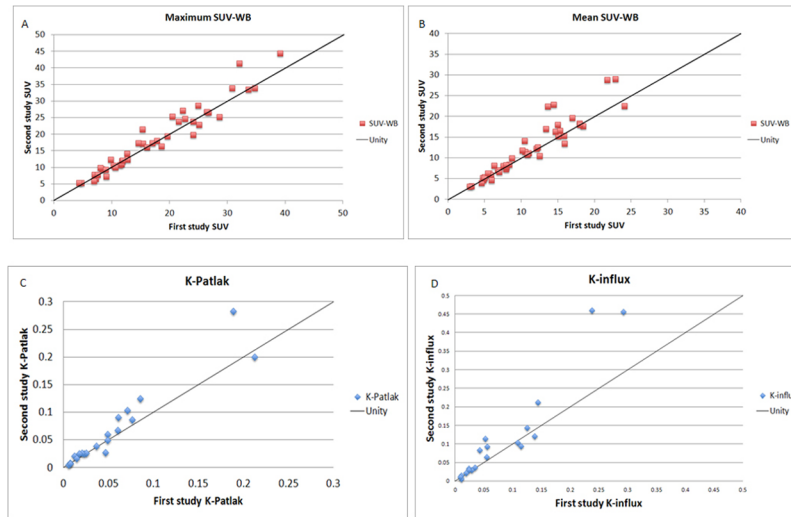


Figure 2. (A–D): Comparison of uptake measurements on first and second ^{68}Ga -DOTATOC PET scan. There is an excellent correlation between two scans for maxSUV, meanSUV, K-Patlak and K-influx. For presentation purposes, 3 lesions with extremely high uptake are not included in the SUV distribution curves and one lesion is excluded in the K-Patlak and K-influx curves.

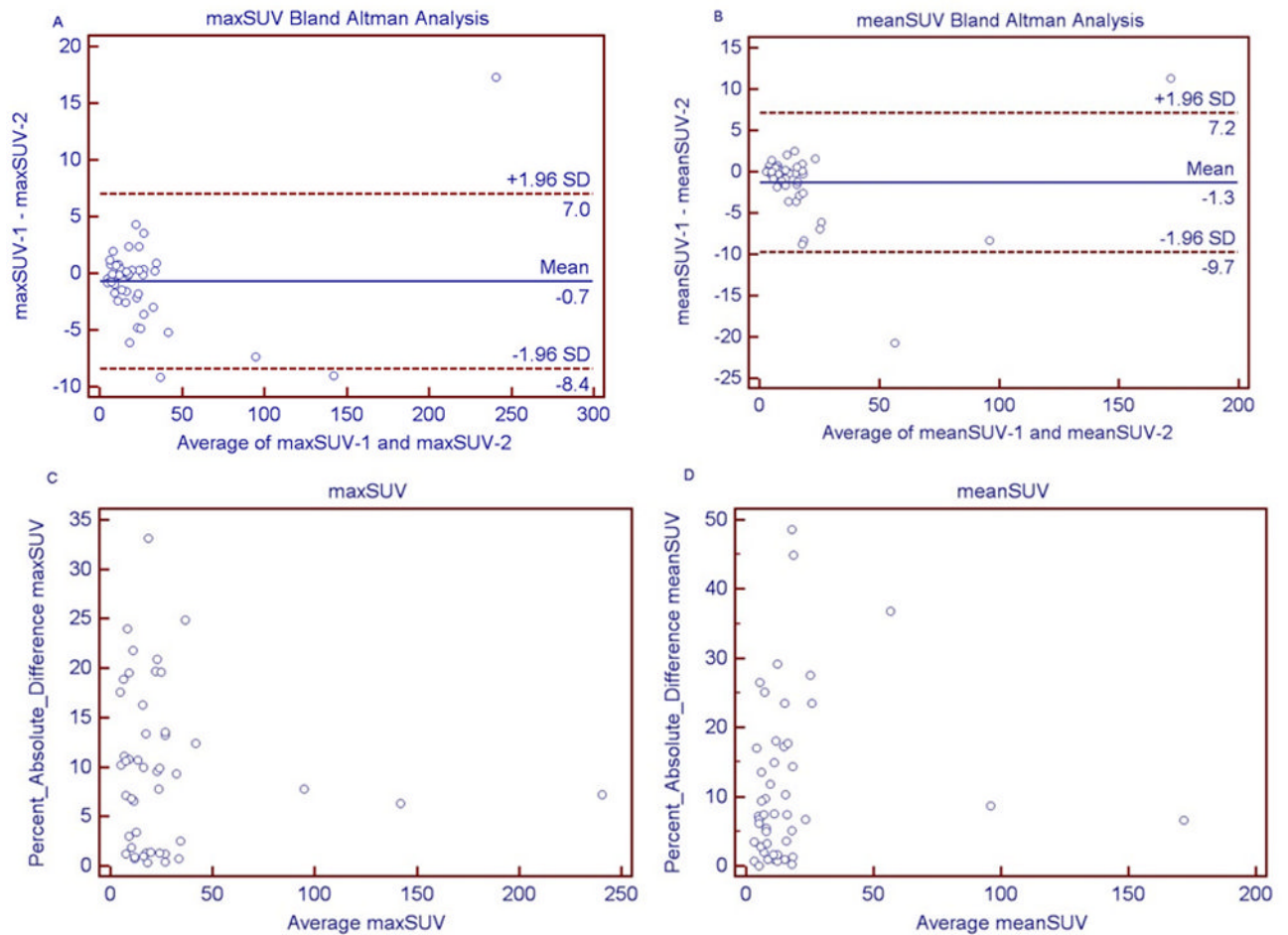


Fig. 3. (A–D): Bland Altman graphs for maxSUV and meanSUV (3A and 3B), which show the correlation of the difference of SUV (SUV1-SUV2) and the average of the SUV in two scans. Figures 3C and 3D show the correlation between absolute percent difference in SUV and the average SUV in two scans. The difference in SUV between two scans was higher in tumors with higher uptake (3A and 3B); the percent differences were however independent from the magnitude of SUV (3C and 3D).

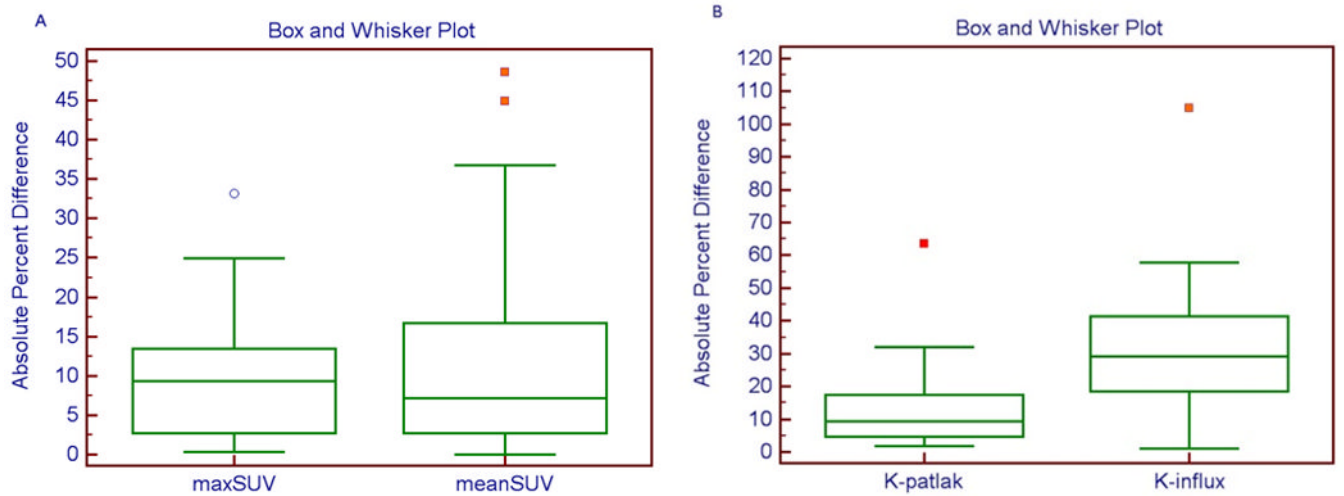


Fig. 4.

(A–B): Box and whisker plot for absolute percent difference for maxSUV and meanSUV from whole body images (Figure 4A) and for kinetic parameters from dynamic data (Figure 4B). Note the outlier values identified using Tukey outlier test. The highest values for absolute percent differences between two scans after exclusion of outliers were 24.9% for maxSUV, 36.8% for meanSUV, 32.0% for K-Patlak and 57.8% for K-influx.

Table 1

Clinical Characteristics of the Patients

	Subject 1	Subject 2	Subject 3	Subject 4	Subject 5
Primary Pathology	Well-differentiated NET, ileal primary	Well-differentiated NET, ileal primary	Well-differentiated NET, pancreatic gastrinoma	Well-differentiated NET, unknown primary	Well-differentiated NET, ileal primary
Symptoms & Biomarkers	Carcinoid Syndrome, elevated serotonin, CgA and pancreastatin	Carcinoid Syndrome, elevated serotonin, CgA and pancreastatin	No symptoms, elevated gastrin	Carcinoid Syndrome, elevated serotonin, CgA and pancreastatin	Carcinoid Syndrome, elevated serotonin, CgA and pancreastatin
Treatment	Octreotide LAR	Octreotide LAR and octreotide SQ; Previous course of everolimus	Octreotide LAR; Previous hepatic chemo- embolization	Octreotide SQ; Previous PRRNT	Octreotide LAR and octreotide SQ

CgA: Chromogranin A SQ: subcutaneous LAR: long-acting release PRRNT: peptide receptor radionuclide therapy

Table 2

Percent Differences for SUV (n=47) and Pharmacokinetic Parameters (n=21)

Parameter	Scan 1	Scan 2	Average Percent Difference [Scan 2 – Scan 1] Mean ± SD	Average Absolute Percent Difference Mean ± SD	Median Absolute Percent Difference Median (IQR)	Intraclass correlation coefficient
meanSUV	17.0 ± 27.6	18.3 ± 27.4	-5.6 ± 15.6%	11.6 ± 11.8%	7.4% (14.1%)	0.99
maxSUV	26.2 ± 40.0	26.9 ± 38.8	-3.4 ± 12.6%	9.75 ± 7.9%	9.3% (10.6%)	0.99
K-Patlak	0.077 ± 0.13	0.090 ± 0.14	4.5 ± 26.2%	20.4 ± 16.4%	12.5% (12.6%)	0.99
K-influx	0.097 ± 0.13	0.158 ± 0.243	15.0 ± 30.4%	25.4 ± 20.6%	29.9% (22.4%)	0.85